Math. Model. Nat. Phenom. 17 (2022) 39
https://doi.org/10.1051/mmnp/2022024

Mathematical Modelling of Natural Phenomena
www.mmnp-journal.org

QUANTIFYING THE EFFECTS OF NON-PHARMACEUTICAL AND PHARMACEUTICAL INTERVENTIONS AGAINST COVID-19 EPIDEMIC IN THE REPUBLIC OF KOREA: MATHEMATICAL MODEL-BASED APPROACH CONSIDERING AGE GROUPS AND THE DELTA VARIANT

Youngsuk Ko[1], Victoria May P. Mendoza[1,2], Yubin Seo[3], Jacob Lee[3], Yeonju Kim[4], Donghyok Kwon[4] and Eunok Jung[1,*]

Abstract. Early vaccination efforts and non-pharmaceutical interventions (NPIs) were insufficient to prevent a surge of COVID-19 cases triggered by the Delta variant. A compartment model that includes age, vaccination, and variants was developed. We estimated the transmission rates using maximum likelihood estimation, and phase-dependent NPIs according to government policies from 26 February to 8 October 2021. Simulations were done to examine the effects of varying dates of initiation and intensity of eased NPIs, arrival timing of Delta, and speed of vaccine administration. The estimated transmission rate matrices show distinct patterns, with transmission rates of younger groups (0–39 years) much larger with Delta. Social distancing (SD) level 2 and SD4 in Korea were associated with transmission reduction factors of 0.63–0.70 and 0.70–0.78, respectively. The easing of NPIs to a level comparable to SD2 should be initiated not earlier than 16 October to keep the number of severe cases below Korea's healthcare capacity. Simulations showed that a surge prompted by Delta can be prevented if the number of people vaccinated daily or SD level when Delta arrived was higher. The timing of easing, intensity of NPIs, vaccination speed, and screening measures are key factors in preventing another epidemic wave.

Mathematics Subject Classification. 92-10, 92B05, 92D30.

Received November 11, 2021. Accepted June 1, 2022.

1. Introduction

The coronavirus disease 2019 (COVID-19) is an ongoing pandemic caused by the severe acute respiratory syndrome coronavirus 2 (SARS-CoV-2). The rise in the number of COVID-19 cases observed worldwide around July 2021 can be attributed to the emergence of the Delta variant of SARS-CoV-2 [19]. The Delta variant

Keywords and phrases: Maximum likelihood estimation, vaccination, social distancing, transmission rate, age-structured.

[1] Department of Mathematics, Konkuk University, Seoul 05029, Korea.
[2] Institute of Mathematics, University of the Philippines Diliman, Quezon City 1101, Philippines.
[3] Division of Infectious Disease, Department of Internal Medicine, Kangnam Sacred Heart Hospital, Hallym University College of Medicine, Seoul 07441, Korea.
[4] Division of Public Health Emergency Response Research, Korea Disease Control and Prevention Agency, Chungcheongbuk-do 28159, Korea.

* Corresponding author: junge@konkuk.ac.kr

significantly reduced the effectiveness of vaccines to symptomatic infection to about 50–70% compared to the Alpha variant [15, 32]. Nevertheless, these vaccines are reported to still be effective against severe disease, hospitalization, and death [1, 15].

To mitigate the spread of COVID-19, on top of vaccination, various non-pharmaceutical interventions (NPIs), such as social distancing (SD), are implemented concurrently. In Korea, a four-level SD plan has been implemented since July 2021. The plan outlines the number of persons allowed in a gathering and operational guidelines of shops, restaurants, gyms, pubs, concert halls, sports stadiums, and other commercial facilities. On 12 July 2021, SD level has been raised to the highest level (SD4) to combat the fourth wave of COVID-19 in the Republic of Korea. As of 29 October 2021, there were 360 536 confirmed cases and 2817 deaths of COVID-19 in Korea [12].

Vaccination in Korea began on 26 February 2021 and priority was given to the healthcare workers and elderly. The vaccination plan proceeded according to age, starting with the older age group [12]. Several types of vaccines have been administered, mostly BNT162b2 and ChAdOx1 [12]. Meanwhile, the first case of a local community transmission in Korea with the Delta variant was reported on 27 April 2021. The number of cases has steeply increased since then and by September 2021, the proportion of the Delta variant among the genome-sequenced COVID-19 cases in Korea is almost 100% [6].

Deterministic models of COVID-19 which incorporated NPIs have been utilized in other studies [20, 28, 38, 40]. Transmission of COVID-19 in various countries has also been successfully described using a deterministic framework [17, 18, 26, 35, 39, 44]. For instance in [26], the age-structured model captured key epidemic features in the UK during the early COVID-19 epidemic in 2020. The model was used to assess the impact of different levels of relaxation of NPIs to epidemic progression, provide short- and long-term predictions, and support for evidence-based policymaking.

The key factors leading the epidemic of COVID-19 recently are vaccination, variants of the virus, and implementation of SD. In this study, we developed an age-structured compartment model that captures COVID-19 transmission with the Delta and non-Delta variants among vaccinated and unvaccinated people. Transmission rates between age groups before and during the period when Delta became the dominant variant of SARS-CoV-2 infections are estimated using maximum likelihood estimation (MLE), which is a preferred parameter estimation and inference tool in statistics [29, 30]. Furthermore, we quantify NPIs according to government policy and present scenarios that investigate the impact of timely vaccination, effective NPIs, and early detection of cases.

2. Materials and methods

2.1. Mathematical model

The model we develop is an extension of the models in [29, 30] to include age-specific transmission rates of the Delta and non-Delta variants. The dynamics of infection with the Delta or non-Delta variants follows an SEIQR scheme, where the subscripts i and v refer to age group and vaccination, respectively, and the superscripts $non\delta$ or δ refer to whether the infection is with the non-Delta or Delta variant, respectively. Compartments for individuals who are vaccinated effectively (V) or ineffectively (U), and then developed partial (P^{part}) or full immunity (P^{full}) are also considered.

The population is divided into eight age groups: those aged 0–17 are referred to as group 1, 18–29 as group 2, and those aged 30–39, 40–49, and so on until 80 and above, are groups 3–8, respectively. The model diagram depicted in Figure 1 shows that susceptible (S) and vaccinated individuals (V, U, P^{part}) may be exposed (E) to non-Delta or Delta variants with a force of infection $\lambda(t)$, and become infectious (I) after $1/\kappa^{non\delta}$ or $1/\kappa^{\delta}$ days. Here we assume that the latent period of infection with the Delta variant is shorter than the non-Delta variant [42, 43]. Once confirmed, infectious individuals are isolated and categorized as mild (Q^m) or severe (Q^s), and eventually recover (R) or die.

The following system of ordinary differential equations describes the developed age-structured model

$$\frac{\mathrm{d}S_i}{\mathrm{d}t} = -(\lambda_i^{non\delta} + \lambda_i^{\delta})S_i - \nu_i,$$

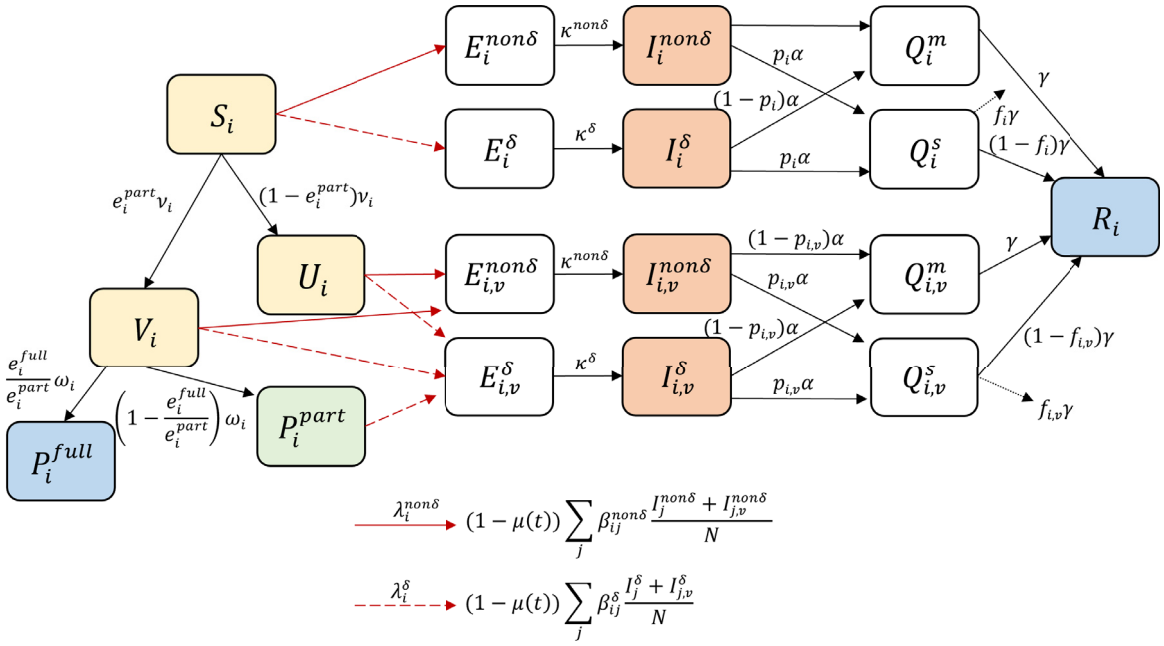

FIGURE 1. The model flowchart describing the transmission of COVID-19 with the non-Delta or Delta variants. The susceptible class of age group i, denoted by S_i, can be exposed to the non-Delta or Delta variants $(E_i^{non\delta}, E_i^{\delta})$ with forces of infection $\lambda_i^{non\delta}$ or λ_i^{δ}, respectively. The transmission reduction factor $\mu(t)$ quantifies the NPIs according to government policy. Also, S_i can become effectively V_i or ineffectively U_i vaccinated, depending on the daily number of vaccinated individuals ν_i, and vaccine effectiveness to the non-Delta variant e_i^{part}. Individuals in V_i become partially P_i^{part} or fully protected P_i^{full} from infection after $1/\omega_i$ days on average, or may be exposed to the non-Delta or Delta variant $(E_{i,v}^{non\delta}, E_{i,v}^{\delta})$. Vaccine effectiveness to the Delta variant is denoted by e_i^{full}. The mean latent period of the non-Delta and Delta variants are $1/\kappa^{non\delta}$ and $1/\kappa^{\delta}$ days, respectively. The mean infectious period is $1/\alpha$ days. Those in the infectious classes $(I_i^{non\delta}, I_i^{\delta}, I_{i,v}^{non\delta}$ and $I_{i,v}^{non\delta})$ are isolated as soon as confirmed, and are classified as mild $(Q_i^m,\ Q_{i,v}^m)$ or severe $(Q_i^s,\ Q_{i,v}^s)$. Individuals in the isolated compartments may die or recover (R_i) after $1/\gamma$ days on average. The parameters $p_i, p_{i,v}$ represent the proportion that becomes severe and $f_i, f_{i,v}$ are the mean fatality rates of the unvaccinated and vaccinated individuals, respectively.

$$
\begin{cases}
\dfrac{\mathrm{d}E_i^{non\delta}}{\mathrm{d}t} = \lambda_i^{non\delta} S_i - \kappa^{non\delta} E_i^{non\delta}, \quad \dfrac{\mathrm{d}E_i^{\delta}}{\mathrm{d}t} = \lambda_i^{\delta} S_i - \kappa^{\delta} E_i^{\delta}, \\
\dfrac{\mathrm{d}E_{i,v}^{non\delta}}{\mathrm{d}t} = \lambda_i^{non\delta}(U_i + V_i) - \kappa^{non\delta} E_i^{non\delta}, \quad \dfrac{\mathrm{d}E_{i,v}^{\delta}}{\mathrm{d}t} = \lambda_i^{\delta}(U_i + V_i + P_i^{part}) - \kappa^{\delta} E_i^{\delta},
\end{cases}
$$

$$
\begin{cases}
\dfrac{\mathrm{d}I_i^{non\delta}}{\mathrm{d}t} = \kappa^{\delta} E_i^{non\delta} - \alpha I_i^{non\delta}, \quad \dfrac{\mathrm{d}I_i^{\delta}}{\mathrm{d}t} = \kappa^{non\delta} E_i^{\delta} - \alpha I_i^{\delta}, \\
\dfrac{\mathrm{d}I_{i,v}^{non\delta}}{\mathrm{d}t} = \kappa^{non\delta} E_{i,v}^{non\delta} - \alpha I_{i,v}^{non\delta}, \quad \dfrac{\mathrm{d}I_{i,v}^{\delta}}{\mathrm{d}t} = \kappa^{\delta} E_{i,v}^{\delta} - \alpha I_{i,v}^{\delta},
\end{cases}
$$

$$
\begin{cases}
\dfrac{\mathrm{d}Q_i^m}{\mathrm{d}t} = \alpha(1-p_i)(I_i^{non\delta} + I_i^{\delta}) - \gamma Q_i^m, \quad \dfrac{\mathrm{d}Q_i^s}{\mathrm{d}t} = \alpha p_i (I_i^{non\delta} + I_i^{\delta}) - \gamma Q_i^s, \\
\dfrac{\mathrm{d}Q_{i,v}^m}{\mathrm{d}t} = \alpha(1-p_{i,v})(I_{i,v}^{non\delta} + I_{i,v}^{\delta}) - \gamma Q_{i,v}^m, \quad \dfrac{\mathrm{d}Q_{i,v}^s}{\mathrm{d}t} = \alpha p_{i,v} (I_{i,v}^{non\delta} + I_{i,v}^{\delta}) - \gamma Q_{i,v}^s,
\end{cases}
$$

$$\frac{\mathrm{d}R_i}{\mathrm{d}t} = \gamma(Q_i^m + (1-f_i)Q_i^s + Q_{i,v}^m + (1-f_{i,v})Q_{i,v}^s),$$
$$\frac{\mathrm{d}U_i}{\mathrm{d}t} = (1-e_i^{part})\nu_i - (\lambda_i^{non\delta} + \lambda_i^{\delta})U_i,$$
$$\frac{\mathrm{d}V_i}{\mathrm{d}t} = e_i^{part}\nu_i - (\lambda_i^{non\delta} + \lambda_i^{\delta})V_i - \omega_i V_i,$$
$$\frac{\mathrm{d}P_i^{part}}{\mathrm{d}t} = \left(1 - \frac{e_i^{full}}{e_i^{part}}\right)\omega_i V_i - \lambda_i^{\delta} P_i^{part},$$
$$\frac{\mathrm{d}P_i^{full}}{\mathrm{d}t} = \frac{e_i^{full}}{e_i^{part}}\omega_i V_i,$$

where the forces of infection $\lambda_i^{non\delta}$ and λ_i^{δ} are defined as

$$\lambda_i^{non\delta}(t) = (1-\mu(t))\sum_{j=1}^{8}\beta_{ij}^{non\delta}\frac{I_j^{non\delta} + I_{j,v}^{non\delta}}{N},$$
$$\lambda_i^{\delta}(t) = (1-\mu(t))\sum_{j=1}^{8}\beta_{ij}^{\delta}\frac{I_j^{\delta} + I_{j,v}^{\delta}}{N},$$

$\mu(t)$ is the phase-dependent, transmission reduction factor accounting for NPIs, $\beta_{ij}^{non\delta}$ and β_{ij}^{δ} are the transmission rates between age groups, and

$$N = \sum_{i=1}^{8}\Big(S_i + E_i^{non\delta} + E_i^{\delta} + E_{i,v}^{non\delta} + E_{i,v}^{\delta} + I_i^{non\delta} + I_i^{\delta} + I_{i,v}^{non\delta} + I_{i,v}^{\delta} + R_i + U_i + V_i + P_i^{part} + P_i^{full}\Big).$$

The age-specific, vaccine-dependent parameters e^{part}, e^{full}, and ω were calculated based on the proportion of an age group vaccinated with either ChAdOx1 or BNT162b2, effectiveness of one or two doses of these vaccines against the Delta and non-Delta variants, and interval between doses. We used the vaccine effectiveness of two doses of ChAdOx1 or BNT162b2 to the non-Delta and Delta variants from [32] (see Table A.1 in Appendix A) to calculate e^{part} and e^{full}. Data on the types of administered vaccines and ages of individuals vaccinated from 26 February to 8 October 2021 were accessed from [5, 10]. Table A.2 in Appendix A shows the proportions of those administered with ChAdOx1 among the vaccinated in each age group. Since we assumed that only two types of vaccines were administered during this period, the proportions who received BNT162b2 can be inferred from the table. Furthermore, the average intervals between doses of ChAdOx1 and BNT162b2 were set to 11 and 4 weeks, respectively, following the Korea Disease Control and Prevention Agency (KDCA) policy [9], and two more weeks were added to these intervals to compute for the average duration to full immunity ($1/\omega$). More details on the calculation of e^{part}, e^{full}, and ω are in Appendix A.

The age-specific mean fatality rates (f, f_v) and proportion of severe cases (p, p_v) for the unvaccinated and vaccinated groups were available from KDCA reports [7, 8].

The transmission rates β for the Delta and non-Delta variants were estimated using MLE from COVID-19 case data including age, date of diagnosis by PCR test, and date of symptom onset from 26 February to 10 September 2021 provided by the KDCA. The parameter $\mu(t)$, which takes a value between 0 and 1, quantifies the NPIs according to government policy. Its value was estimated from the cumulative case data using least-squares fitting. A μ value close to 1 means stricter NPIs while a value close to 0 means more relaxed policies. Data on the number of individuals vaccinated per day (η) is available in [2]. Tables 1 and 2 summarize the age-specific and non-age-specific model parameters and their values.

TABLE 1. Non-age-specific parameters of the model.

Symbol	Description	Value	Reference
$1/\kappa^{non\delta}$	Mean latent period of the non-Delta variant	4 days	[42, 43]
$1/\kappa^{\delta}$	Mean latent period of the Delta variant	2 days	[42, 43]
$1/\alpha$	Mean infectious period	6 days	[27, 43]
$1/\gamma$	Mean duration of isolation (hospitalization)	20 days	[31]

TABLE 2. Age-specific parameters of the model calculated using data from [5, 9] and vaccine effectiveness from [32]. The age-specific fatality rates and severity for the vaccinated and unvaccinated groups were available from KDCA reports [7, 8].

		Age group							
Symbol	Description	1	2	3	4	5	6	7	8
p_i	Proportion of unvaccinated group i that becomes severe	0	0	0.01	0.02	0.04	0.07	0.13	0.26
$p_{i,v}$	Proportion of vaccinated group i that becomes severe	0	0	0	0.01	0.01	0.03	0.02	0.05
f_i	Mean fatality rate of unvaccinated group i (1/day)	0	0	0	0	0	0.01	0.06	0.20
$f_{i,v}$	Mean fatality rate of vaccinated group i (1/day)	0	0	0	0	0	0.01	0.06	0.20
e_i^{part}	Vaccine effectiveness to non-Delta	0.94	0.93	0.91	0.9	0.91	0.76	0.83	0.92
e_i^{full}	Vaccine effectiveness to Delta	0.88	0.87	0.85	0.84	0.85	0.69	0.76	0.86
$1/\omega_i$	Mean interval from first dose to immunity (1/day)	33.26	34.18	37.85	39.69	37.24	61.73	50.10	36.63

2.2. Maximum likelihood estimation

We apply MLE to estimate the transmission rates of the Delta and non-Delta variants between age groups by considering two periods. Transmission rates of the non-Delta variant were estimated from the period 26 February to 30 June 2021, while the data from 1 August to 10 September, when the proportion of cases with the Delta variant was over 80%, were used to estimate the transmission rates for the Delta variant [16].

To establish the likelihood function to be optimized, we first divide each age group into three subgroups to distinguish COVID-19 outcomes: infected (Λ_{Ii}), unvaccinated and uninfected (Λ_{Si}), and effectively vaccinated and uninfected (Λ_{Vi}), where i indicates the age group. Let β_{XY} be the transmission rate from age group Y to X. Assuming a homogeneous mixing of the population, and that the transmission events are exponentially distributed, the probability that an individual x in subgroup Λ at the time $t-1$ is still uninfected until the next time t is given by

$$p_{S,\Lambda,x}(t) = exp\left(-\frac{\sum_j \beta_{ij}\mathbf{I}_j(t-1)}{N}\right),$$

where $\mathbf{I}_j(t-1)$ denotes the number of hosts in group j which can spread the disease at time $t-1$, and N is the total population. We can set N as a constant because the number of isolated individuals (or deceased) is less than 0.02% of the population. On the other hand, the probability that an individual x in group Λ is uninfected at the time $t-1$ but becomes infected at t is

$$p_{I,\Lambda,x}(t) = 1 - exp\left(-\frac{\sum \beta_{ij}\mathbf{I}_j(t-1)}{N}\right).$$

Hence, an individual who stays uninfected until final time t_f has probabilities $p_{S,\Lambda,x}(t)$ at each time until t_f. In addition, an individual can be vaccinated at time $t_{Vi,x}$, have immunity after $t_{e,i}$ days, and stay uninfected until final time t_f. An individual infected at time $t_{Ii,x}$ has probabilities $p_{S,\Lambda,x}(t)$ until $t_{Ii,x}-1$ and $p_{Ii,\Lambda,x}(t_{Ii,x})$.

The likelihood function L is formulated as

$$L = \prod_i \left(L_{1,i} \cdot L_{2,i} \cdot L_{3,i}\right),$$

where

$$\begin{aligned}
L_{1,i} &= \prod_{x\in\Lambda_{Si}} \left(\prod_{t=0}^{t_f} p_{Si,x}(t)\right),\\
L_{2,i} &= \prod_{x\in\Lambda_{Vi}} \left(\prod_{t=0}^{\min\{t_f, t_{Vi,x}+t_{e,i}\}} p_{S,\Lambda_{Vi},x}(t)\right),\\
L_{3,i} &= \prod_{x\in\Lambda_{Ii}} \left(\prod_{t=0}^{t_{Ii,x}-1} p_{S,\Lambda_{Ii},x}(t)\right) p_{I,\Lambda_{Ii},x}(t_{Ii,x}).
\end{aligned}$$

By taking the logarithm of L and using the optimization toolbox in MATLAB, we obtain a matrix containing the transmission rates of the Delta and non-Delta variants between age groups.

2.3. Parameter bootstrapping and sensitivity analysis

In this study, we perform parameter bootstrapping for the estimated NPIs-related reduction factors ($\mu(t)$). Parameter bootstrapping is a statistical technique for quantifying uncertainty and constructing confidence intervals of estimated parameters. The algorithm generates large samples of synthetic data sets using the estimated model parameters assuming a certain probability distribution structure. Here we adopt the algorithm introduced in [23]. We sampled 10,000 synthetic data sets having Poisson distribution and the parameters are re-estimated from the generated data sets. The means, medians, standard deviations, and 95% confidence intervals of the re-estimated parameters are calculated.

Mathematical models contain various input parameters wherein each parameter affects the model outputs. Sensitivity analysis can be implemented to measure the correlation between parameters (input) and model output (such as number of cases). The partial rank correlation coefficient (PRCC) is one of the most reliable sensitivity analysis methods and can be applied when the input and output has nonlinear but monotone relation [34]. Further description about the algorithm for calculating PRCC is presented in [34].

Six epidemiological parameters were selected for PRCC, the factors for the transmission rates of the non-Delta and Delta variants ($\beta^{non\delta}, \beta^{\delta}$), mean latent period of the non-Delta and Delta variants ($1/\kappa^{non\delta}, 1/\kappa^{\delta}$), mean infectious period ($1/\alpha$), and severity rate adjusting constant (p). Note that there are eight transmission rates each for the non-Delta and Delta variants, and severe rates p_i, one for each age group. The parameter p is a constant factor that affects each p_i. For example, if p is 0.5, this means that the severity rates for each age group becomes half of its original value. In the same way, the parameters $\beta^{non\delta}$ and β^{δ} are the factors affecting

transmission rates. We set the input parameters to be uniformly distributed on a bounded range, and sampling was performed independently. The cumulative numbers of incidence and severe cases from 20 days to 220 days ($t = 20$ to $t = 220$), and every 20 days after the start of the simulation, are considered as model outputs. The PRCC method was performed 10,000 times. Note that the arrival time of the δ variant in the local community is 52 days after the initiation of simulation.

2.4. Normalization of the transmission rate matrices and the effective reproductive number

Various NPIs, including SD, were implemented by the government during the periods used in estimating the transmission rates. To exclude these phase-dependent components and distinguish the transmission rates from the reduction factor due to NPIs $\mu(t)$, we normalize the transmission rate matrices. Let the transmission rate matrices estimated from 26 February to 30 June and from 01 August to 10 September be $M_{est}^{non\delta}$ and M_{est}^{δ}, respectively. First, calculate the reproductive number of COVID-19 using $M_{est}^{non\delta}$ *via* the next-generation matrix method, which is described in Appendix B, and denote this as $\mathcal{R}_{est}^{non\delta}$. Then the normalized transmission rate matrix of the non-Delta variant $M^{non\delta}$ is formulated as

$$M^{non\delta} = M_{est}^{non\delta} \frac{\mathcal{R}_0^{non\delta}}{\mathcal{R}_{est}^{non\delta}},$$

where $\mathcal{R}_0^{non\delta}$, equal to 3.17, is the basic reproductive number of COVID-19 estimated from various studies before Delta variant became the major strain [21]. Similarly, the normalized transmission rate matrix of the Delta variant M^{δ} is formulated as

$$M^{\delta} = M_{est}^{\delta} \frac{\mathcal{R}_0^{\delta}}{\mathcal{R}_{est}^{\delta}},$$

where $\mathcal{R}_{est}^{\delta}$ is reproductive number calculated using M_{est}^{δ} and $\mathcal{R}_0^{\delta} = 1.97\mathcal{R}_0^{non\delta}$ [22]. The normalized transmission rate matrices, $M^{non\delta}$ and M^{δ}, are used in this research.

The effective reproductive number $\mathcal{R}_t$ is a time-dependent measure of the average number of secondary cases from a single infectious individual [36]. In this study, $\mathcal{R}_t$ is calculated using the next-generation matrix method. Using the normalized transmission rate matrices, $\mathcal{R}_t$ of the non-Delta and Delta variants are 3.17 and 6.24, respectively, if there are no NPIs and behavior change.

2.5. Modeling scenarios

To examine the impact of vaccination rollout, we extended the model simulation until 30 December 2021 and analyzed the effect of easing NPIs at different times. Considering that approximately 77% of the population already have at least one dose, we assumed that 85% of the population is vaccinated by 30 November 2021. We consider three dates for the initiation of eased NPIs: 8 October, 18 October, and 1 November. For each date, we simulate three scenarios with different values of the transmission reduction factor $\mu(t)$: $\mu = 0.69$ in scenario 1 (S1), $\mu = 0.64$ in scenario 2 (S2), and $\mu = 0.52$ in scenario 3 (S3). The value of μ in S3 was estimated from the third epidemic wave in 2020, when it was SD1, and is a relatively lower value compared to the μ in S2 [13]. A lower value of μ is associated to more eased NPIs.

We also proceeded with a simulation-based experiment to study the effects of varying the speed of vaccination, arrival timing of the Delta variant, and intensity of NPIs. The initial condition in the simulations is identical to 26 February 2021 in Korea and the simulation time is set to 365 days. The total number of vaccinated people is assumed to be 40 million, which is approximately 78% of the population in Korea, and the number of people vaccinated daily is set to 150,000, 200,000, or 400,000. Moreover, we fix the order of vaccination from oldest to youngest, that is, 8-7-6-5-4-3-2, excluding group 1. We denote by t_δ the day when the individuals exposed to the Delta variant arrived in the local community, and we set its range from zero to 80 days. Note that in Korea,

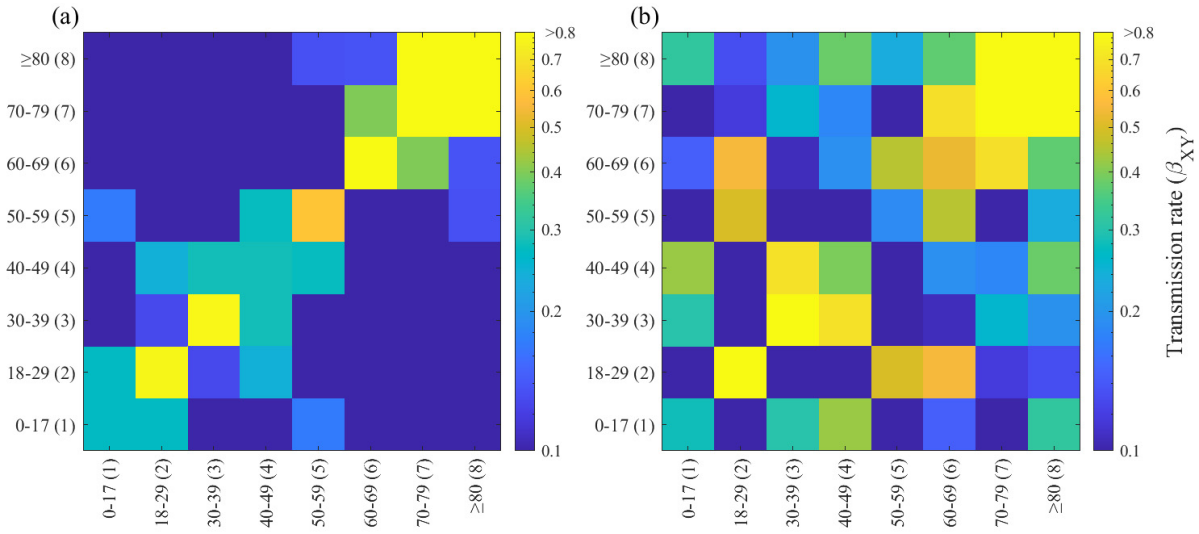

FIGURE 2. Estimated transmission rates between age groups in Korea for the (a) non-Delta variant using data from 26 February to 30 June 2021 and (b) Delta variant using data from 1 August to 10 September 2021.

the date of arrival of the Delta variant corresponds to $t_\delta = 52$. We consider values of μ from 0.52 to 0.78 in 0.001 increments. In total, there are 21 141 simulations for the different values of ν_i, t_δ, and μ.

3. RESULTS

3.1. Parameter estimation

The estimated transmission rates obtained using MLE form a matrix according to the age groups. The transmission rate matrices, visualized in Figure 2, represent the transmission patterns of the non-Delta (a) and Delta variants (b) in Korea.

We use the normalized transmission rate matrices in estimating $\mu(t)$, which is related to the reduction in transmission induced by NPIs according to government policy. The estimates for μ on each phase from 26 February to 8 October 2021 is shown in Table 3. The phases correspond to the government's pronouncement on SD level. Figure 3a shows the plots of the estimates for the reduction factor $\mu(t)$ (red curve) with the effective reproductive number ($\mathcal{R}_t$, blue curve). At the start of the simulation period, Seoul Capital Area was at SD2. When $\mu(t)$ increased from 0.63 to 0.69 around 16 April 2021, $\mathcal{R}_t$ decreased to 0.97 and stayed below 1 until around 16 June. From 16 June to 11 July, μ was estimated at 0.64 and $\mathcal{R}_t$ jumped to as high as 1.52. The exponential rise in the proportion of cases infected with the Delta variant (black solid curve in Fig. 3a) and daily confirmed cases (Fig. 3b) was also observed on the same period, which prompted the start of the fourth wave. On 12 July, the Korean government raised the SD level in Seoul Capital Area to SD4. A steep increase in the cumulative confirmed cases was seen beginning 12 July (Fig. 3c), and the estimates for μ were the highest from this period until 06 September. At the same time, the proportion of hosts having full immunity (black dashed curve in Fig. 3a) increased steadily, reaching up to about 50% by the end of the estimation period. On the last phase, the estimated value of μ was 0.70. The fit of the model to the data on cumulative severe cases and cumulative deaths are shown in Figure 3d and e.

To illustrate how μ can be used to suggest appropriate SD level, assume that the basic reproductive number of the disease is five, Delta and non-Delta variants can infect the population, 80% of population is vaccinated, and vaccine effectiveness is 62.5%. Then without NPIs, $\mathcal{R}_t = 5 \times 0.8 \times 0.625 = 2.5$. To maintain an $\mathcal{R}_t$ below one, SD2 is appropriate since the minimum estimated value of $\mu(t)$ on SD2 was 0.64 and this translates to

TABLE 3. Estimates for the phase-dependent, transmission reduction factor $\mu(t)$, social distancing (SD) level, and range of effective reproductive number $\mathcal{R}_\mathbf{t}$ from 26 February to 8 October 2021.

Phase	Period	$\boldsymbol{\mu(t)}$	SD Level	$\boldsymbol{\mathcal{R}_t}$
1	26 Feb to 25 Mar	0.63	2	[1.15, 1.16]
2	26 Mar to 15 Apr	0.64	2	[1.13, 1.14]
3	16 Apr to 3 Jun	0.69	2	[0.96, 0.98]
4	4 Jun to 15 Jun	0.70	2	[0.94, 0.97]
5	16 Jun to 11 Jul	0.64	2	[1.18, 1.52]
6	12 Jul to 25 Jul	0.76	4	[1.02, 1.08]
7	26 Jul to 8 Aug	0.76	4	[1.06, 1.06]
8	9 Aug to 5 Sep	0.78	4	[0.92, 1.00]
9	6 Sep to 19 Sep	0.70	4	[1.12, 1.23]
10	20 Sep to 8 Oct	0.70	4	[0.94, 1.10]

TABLE 4. Values of the means, medians, standard deviations (SD), and 95% confidence intervals (CI) of the re-estimates of μ on each of the 10 phases from 26 February to 8 October 2021.

Phase	Estimate	Median of estimates	Mean of estimates	SD	95% CI
1	0.6323	0.6327	0.6326	0.0005	[0.6315, 0.6333]
2	0.6373	0.6385	0.6388	0.0011	[0.6373, 0.6410]
3	0.6904	0.6904	0.6905	0.0002	[0.6903, 0.6911]
4	0.7030	0.7024	0.7024	0.0010	[0.7005, 0.7038]
5	0.6411	0.6411	0.6411	0.0005	[0.6400, 0.6419]
6	0.7615	0.7613	0.7612	0.0009	[0.7594, 0.7630]
7	0.7641	0.7644	0.7642	0.0010	[0.7619, 0.7661]
8	0.7769	0.7774	0.7773	0.0007	[0.7758, 0.7785]
9	0.7010	0.7004	0.7006	0.0026	[0.6959, 0.7064]
10	0.7006	0.7004	0.7004	0.0045	[0.6920, 0.7094]

$\mathcal{R}_t = (1 - 0.64) \times 2.5 = 0.9$. On the other hand, if $\mu = 0.52$, which corresponds to the worst case during SD1, then $\mathcal{R}_t = (1 - 0.52) \times 2.5 = 1.2$. Furthermore, SD4 may not be necessary and may aggravate present economic problems.

In Figure 4, we present the best fit of the model to the data on daily and cumulative cases per age group. The rise in the number of cases from 16 June 2021 observed across all age groups was followed by the model, with ages 18–29 having the most and the elderly groups having the least increase. Moreover, the model shows a peak (460 cases) on 16 August and another peak (527 cases) on 28 September in ages 18–29. Towards the end of the simulation period, a decreasing trend in the number of cases was observed in most age groups except ages 0–17, who are not vaccinated.

3.2. Bootstrapping and PRCC results

Figure 5 shows the distribution of the re-estimates of μ on the 10 phases from 26 Feb to 8 Oct 2021. The values of the means, medians, standard deviations (SD), and 95% confidence intervals (CI) are summarized in Table 4. We see that in all cases, the means and medians of the re-estimates lie within the 95% confidence intervals.

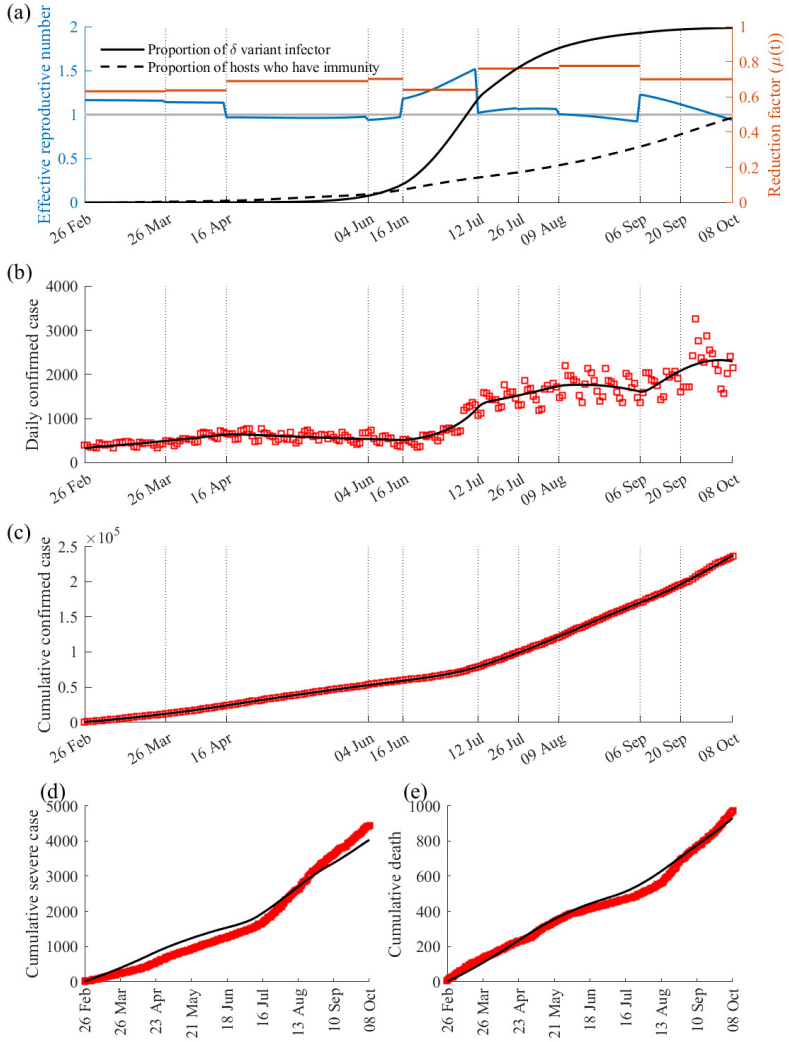

FIGURE 3. The parameter estimation results obtained by fitting the model to the cumulative confirmed cases. Panel (a) shows the effective reproductive number (blue), estimates of the transmission reduction factor $\mu(t)$ (red), proportion of the active cases infected with the Delta variant (black solid curve), and proportion of the total population who has immunity (black dashed curve). The best fit of the model to the (b) daily confirmed cases, (c) cumulative confirmed cases, (d) cumulative severe cases, and (e) cumulative deaths are also shown. The red boxes represent data from 26 February to 8 October 2021.

Figure 6 shows the PRCC values of $\beta^{non\delta}, \beta^{\delta}, 1/\kappa^{non\delta}, 1/\kappa^{\delta}, 1/\alpha$, and p with respect to the cumulative cases (left) and cumulative severe cases (right) on different time points. Both plots show a similar trend of PRCC values except for the parameter p, which is naturally more influenced by the number of severe cases. Table 5 lists the range of PRCC values and time points (in days) when the maximum and minimum PRCC values occurred with respect to the outputs cumulative incidence and severe cases. The $p-$values of the inputs were below 0.01 except for Delta-related parameters before the Delta variant arrived in the local community, and p when the output is cumulative incidence.

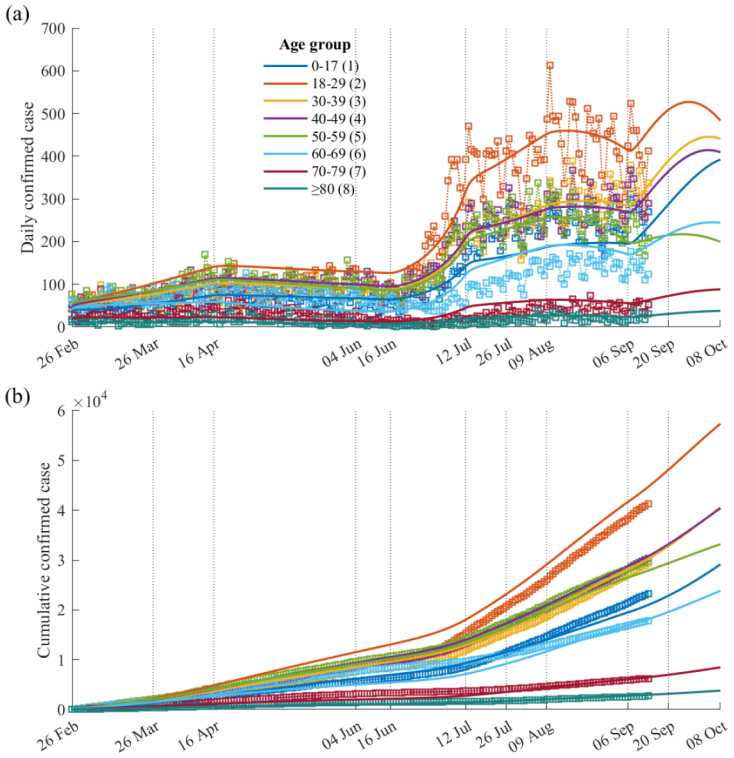

FIGURE 4. The best fit of the model to the (a) daily confirmed cases and (b) cumulative confirmed cases per age group. The boxes represent the data per age group from 26 February to 10 September 2021.

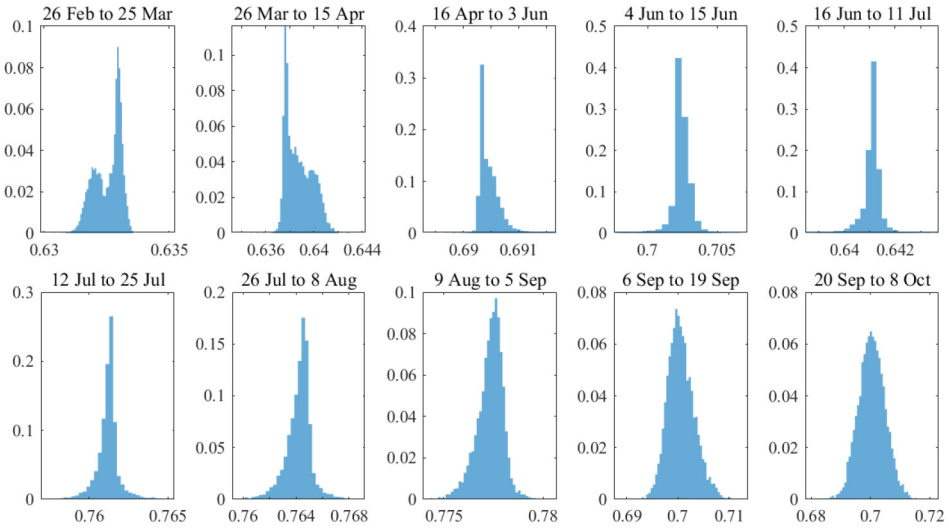

FIGURE 5. The distribution of the re-estimates of μ on each of the 10 phases from 26 February to 8 October 2021.

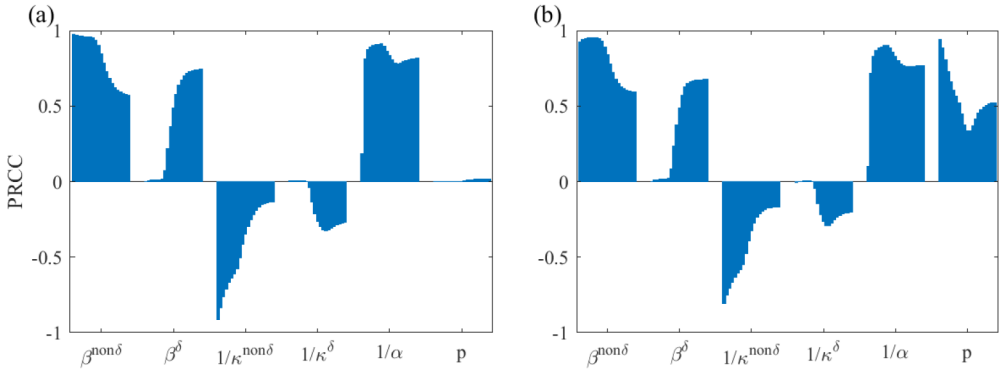

FIGURE 6. Partial rank correlation coefficients (PRCC) for the parameters $\beta^{non\delta}$, β^{δ}, $1/\kappa^{non\delta}$, $1/\kappa^{\delta}$, $1/\alpha$, and p every 20 days starting from day 20 until day 220 with respect to the outputs (a) cumulative incidence and (b) cumulative severe cases.

TABLE 5. Range of the partial rank correlation coefficients (PRCC) for the parameters $\beta^{non\delta}$, β^{δ}, $1/\kappa^{non\delta}$, $1/\kappa^{\delta}$, $1/\alpha$, and p, and time points (in days) when the maximum and minimum PRCC (in absolute values) occurred with respect to the outputs, cumulative incidence and severe cases.

Parameter	Range of PRCC	Time point of maximum absolute PRCC (day)	Time point of minimum absolute PRCC (day)
$\beta^{non\delta}$	$[0.57, 0.97]$, incidence $[0.58, 0.95]$, severe case	20, incidence 20, severe case	220, incidence 220, severe case
β^{δ}	$[0.00, 0.74]$, incidence $[0.00, 0.67]$, severe case	220, incidence 220, severe case	20, incidence 20, severe case
$1/\kappa^{non\delta}$	$[-0.91, -0.13]$, incidence $[-0.81, -0.18]$, severe case	20, incidence 20, severe case	220, incidence 220, severe case
$1/\kappa^{\delta}$	$[-0.33, 0.00]$, incidence $[-0.29, 0.01]$, severe case	150, incidence 140, severe case	80, incidence 30, severe case
$1/\alpha$	$[0.20, 0.91]$, incidence $[0.11, 0.91]$, severe case	90, incidence 90, severe case	20, incidence 20, severe case
p	$[-0.01, 0.01]$, incidence $[0.33, 0.94]$, severe case	100, incidence 20, severe case	220, incidence 130, severe case

3.3. Analysis on the timing of easing the NPIs

Nine scenarios considering different dates of initiation and levels of eased NPIs are displayed in Figure 7. The red, black, and blue curves, correspond to starting the eased NPIs on 8 October, 18 October, and 1 November 2021, respectively. The solid curves represent S1, dashed curves S2, and dotted curves S3. Panel (a) shows $\mathcal{R}_t$, (b) the daily confirmed cases, (c) the number of severe patients requiring hospital beds, and (d) the cumulative death. The dashed grey curve in panel (c) marks the maximum number of hospital beds (1,067) for severe patients in Korea [14]. Results show that the worst case scenario is S3 with 8 October as easing time, wherein the peak number of daily cases, severe patients, and cumulative deaths could reach 8,479, 1,658, and 1,638, respectively. But if the easing to S3 was started later, on 18 October or 1 November, the peak numbers could be reduced to 4,633 (45% reduction) or 1,963 (77% reduction) for the peak daily cases, 920 (45% reduction) or no increase for the peak number of severe patients, and 969 (41% reduction) or 549 (66% reduction) for the cumulative deaths, compared to when the easing was initiated earlier. The rest of the simulations show a decreasing trend of daily

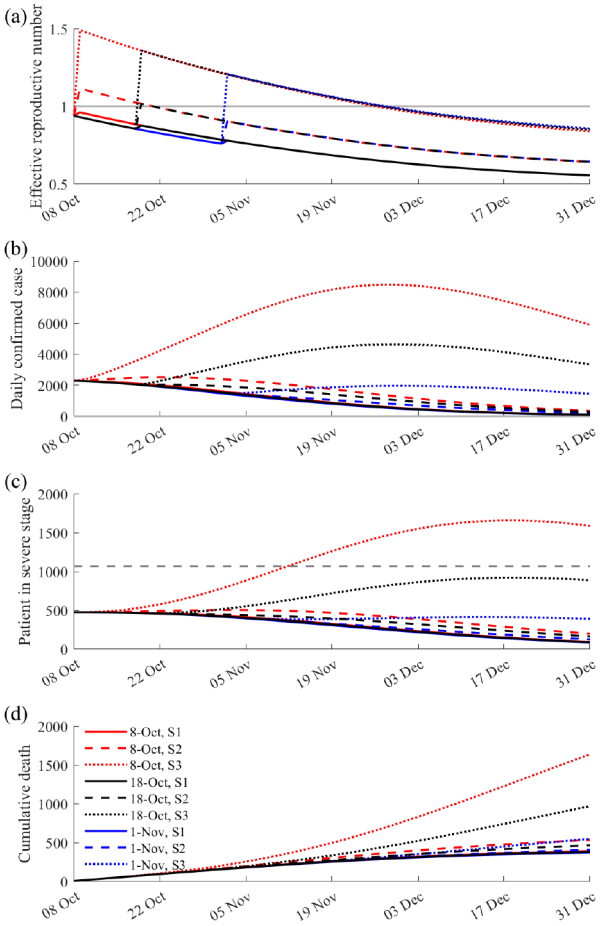

FIGURE 7. Results on the effect of easing NPIs at different times. Panel (a) shows the effective reproductive number, (b) number of daily confirmed cases, (c) number of severe patients requiring hospital beds, and (d) cumulative number of deaths. Colors and shapes of curves indicate the timing of initiation (8 October, 18 October, and 1 November) and level of eased NPIs (S1, S2, and S3). Gray dashed line in (c) indicates the number of available beds (1,067) for severe patients in Korea.

confirmed cases and number of severe patients. The simulations illustrate the importance of the timing of easing NPIs in preventing the occurrence of another epidemic wave. All scenarios, except the worst case, show that the number of severe patients did not reach the limit (1,067) of Korea.

3.4. Analysis on the vaccination speed, NPIs, and arrival timing of the Delta variant

Figure 8 displays the simulation results when initial $\mathcal{R}_t = 1.04$ or 1.14, $t_\delta = 52$, and $\nu_i = 200,000$ or $400,000$. In panel (a), $\mathcal{R}_t$ and the proportion of cases infected with the Delta variant are displayed. The magenta asterisk indicates $t_\delta = 52$. If $\mathcal{R}_t$ is initially 1.04, $\mathcal{R}_t$ increased further up to 1.29 when $\nu_i = 200,000$ (light orange), while it decreased below one if $\nu_i = 400,000$ (light green). Similarly, if initial $\mathcal{R}_t = 1.14$, $\mathcal{R}_t$ increased to 1.42 with $\nu_i = 200,000$ (dark orange) and decreased below one if $\nu_i = 400,000$ (dark green). In panels (b) and (c), a second peak with more than 21,000 cases and 5,700 severe patients is observed when $\nu_i = 200,000$ and initial $\mathcal{R}_t = 1.14$ (dark orange), whereas no second peak is observed when $\nu_i = 400,000$ (green-colored curves).

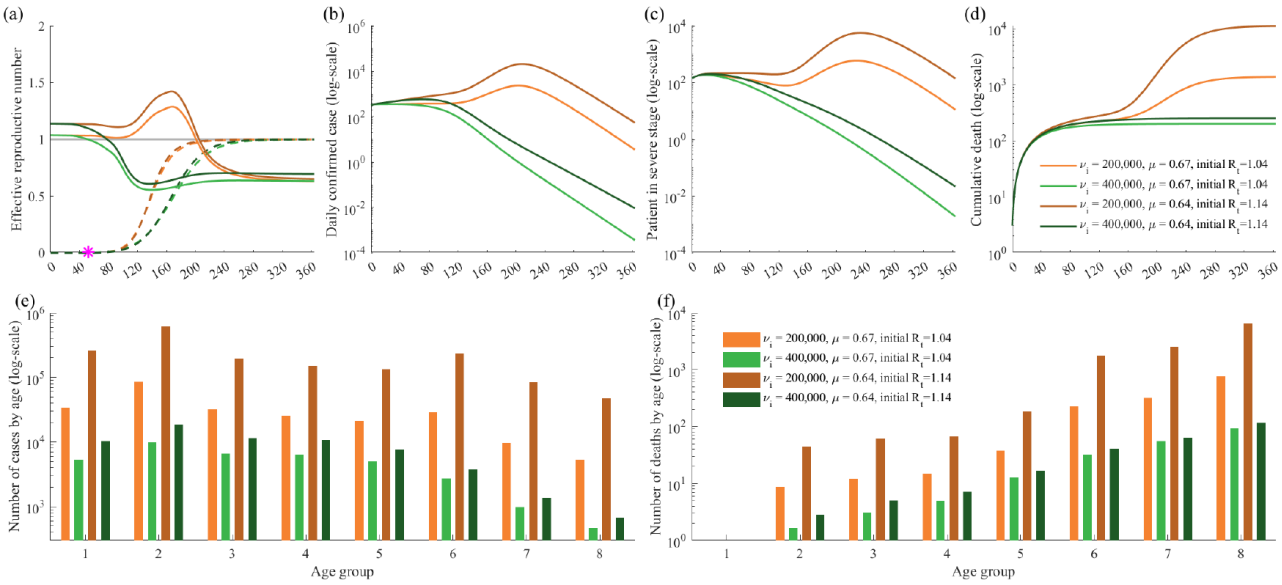

FIGURE 8. The simulation result with initial $\mathcal{R}_t = 1.04$ or 1.14, $t_\delta = 52$, and daily number of vaccination set to 200,000 or 400,000. Panel (a) shows the effective reproductive number, (b) number of daily confirmed cases, (c) number of severe patients requiring hospital beds, (d) cumulative number of deaths, (e) age-dependent number of confirmed cases, and (f) age-dependent number of deaths. Orange-colored and green-colored curves means that the number of daily administered vaccines is 200,000 and 400,000, respectively.

Panel (d) shows that the cumulative deaths when $\nu_i = 200,000$ can reach more than 1,000 compared to when $\nu_i = 400,000$ (below 300). Panels (e) and (f) display the cumulative number of cases and deaths of each age group, with 36% of the cases occurring in age group 2 and 58% of the deaths occurring in age group 8 when $\nu_i = 200,000$ and initial $\mathcal{R}_t = 1.14$. These results highlight the effect of the daily number of vaccination to the occurrence of another epidemic wave.

Figure 9 shows a heat map summarizing the results of the 21,141 simulations. The columns represent the daily vaccination number ($\nu_i = 150,000$, $200,000$, and $400,000$) and the rows correspond to the number of confirmed cases, deaths, and peak number of severe patients requiring hospital beds. In each panel, the x axis represents t_δ and the y axis corresponds to μ. The dotted red curve in panels (g), (h), and (i) marks the maximum number of hospital beds (1,067) for severe patients in Korea.

4. Discussion

The transmission rate matrices of the Delta and non-Delta variants obtained in this study were apparently different among age groups. The transmission rate with non-Delta variant was high between the same age groups. However, transmission with the Delta variant was much higher among age groups of 18-29 and 30-39, and an increased transmission was observed between those age groups and age groups of 50-59 and 60-69. These matrices reflect the distinct epidemiologic characteristic of COVID-19 epidemic after Delta became the dominant variant of SARS-CoV-2 in Korea: 1) incidence in younger age groups, those in 20s and 30s, increased; 2) and the major source of transmission moved from group-related or institutional outbreaks to individual contacts [4, 45]. These results indicate an increased transmission with Delta variant among household contacts, which is coherent with previous studies [24, 33].

Higher transmission rates with the Delta variant compared to the non-Delta variant were also observed in the elderly groups, which may have resulted from breakthrough infections in nursing homes and assisted living

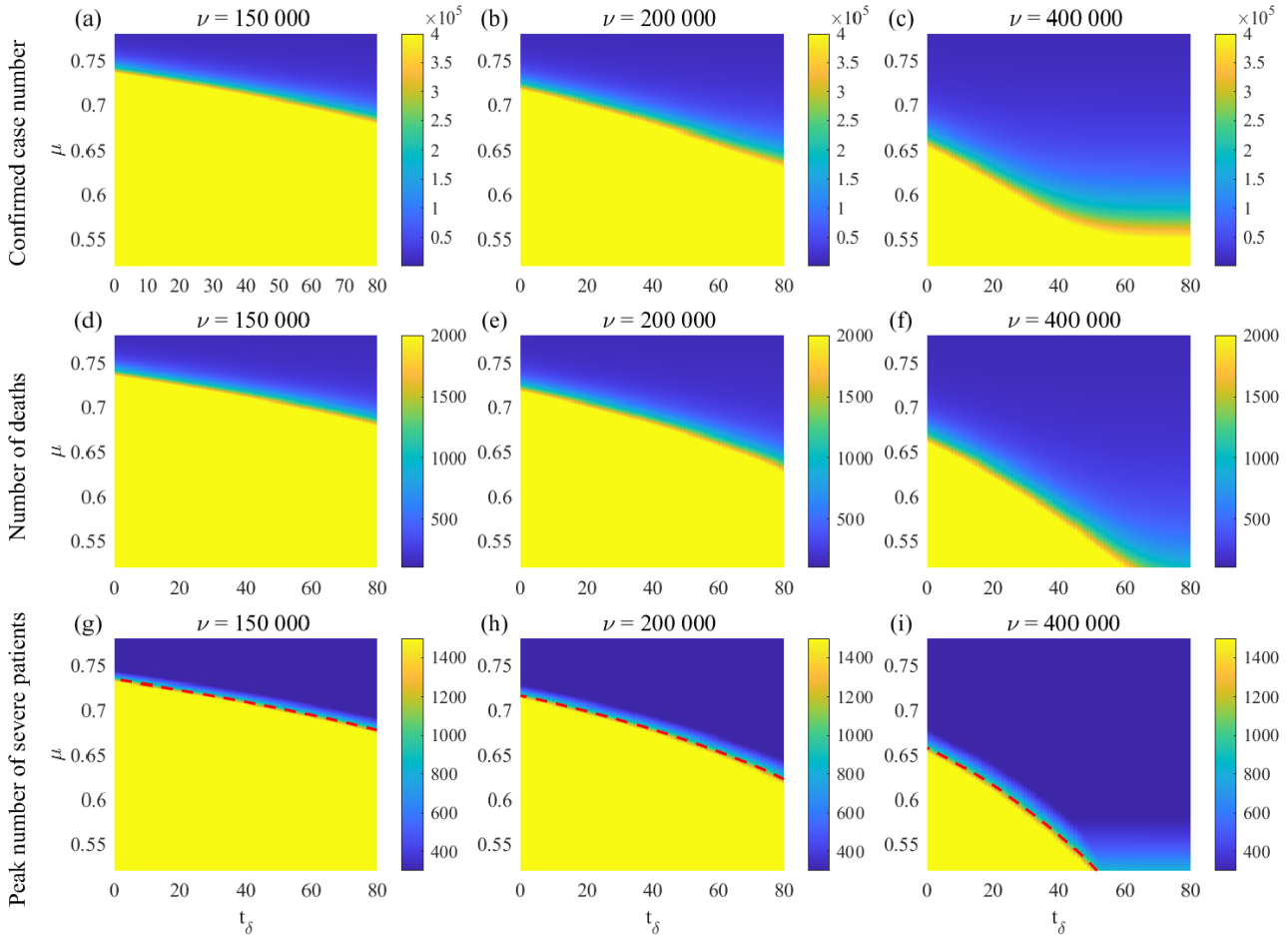

FIGURE 9. The simulation results of the 21,141 runs. The columns from left to right indicate the number of daily administered vaccines as 150,000, 200,000, and 400,000, respectively. Panels (a), (b), and (c) show the number of confirmed cases; (d), (e), and (f) the number of deaths; and (g), (h), and (i) the peak number of severe patients requiring hospital beds. Note that red dotted curve in panels (g), (h), and (i) indicates the maximum number of available beds (1,067) for severe patients in Korea.

facilities [8]. With the absence of vaccination, a much higher transmission rate with the Delta variant was expected, but was not observed in the youngest age group of 17 years old and below. This phenomenon was probably a consequence of the Korean government policy on limiting the number of attendance in school to two-thirds since October 2020 [11]. According to the data, among all the COVID-19 cases of those aged 17 years old and below in Korea, only about 15% were infected from schools during this period [25].

We also analyzed the reduction in transmission induced by NPIs according to government policies, denoted by $\mu(t)$. SD2 and SD4 in Korea corresponded to $\mu(t)$ values from 0.63 to 0.70 and from 0.70 to 0.78, respectively. Values of $\mu(t)$ close to 0.7 may represent SD3 in Korea. Considering the basic reproductive number of a disease, vaccine effectiveness, and amount of administered vaccines, the fitted values of $\mu(t)$ can be an effective measures of the government policy. This parameter would be informative to the healthcare professionals and policy makers on designing prevention and control measures for emerging or reemerging infectious diseases.

Bootstrapping results for the parameter μ showed that the re-estimates lie within narrow ranges from the estimates for the best model fit. Higher PRCC values of the non-Delta-related parameters were observed until

around day 160, approximately 100 days after Delta variant arrived, after which the Delta-related parameters became more sensitive with respect to the cumulative incidence and severe cases. The mean infectious period $1/\alpha$ was shown to be sensitive to both outputs throughout the simulation time, while the factor p is expectedly more sensitive to the cumulative severe cases than the cumulative incidence.

Considering both the medical and economic impact of NPIs, the Korean government plans to reduce SD, termed 'Back to normal or With-Corona', on 1 November 2021 [14]. Because vaccination and immunization takes time, we explored the effect of delaying the initiation of eased SD in Figure 7. When SD was eased to a minimal value (S3), no large-scale re-emergence of infections was observed when S3 was delayed to 1 November, as opposed to when it was initiated on 8 or 18 October. In other words, gradually easing NPIs might be necessary when implementation is earlier. For example, in Korea, the maximum number of people allowed in a private gathering after 6:00PM became four (ten for fully vaccinated) from two since 18 October, although SD remained at SD4 [3].

In our simulations on the effects of vaccination and NPIs, the larger reduction of transmission factor ($\mu(t)$) and faster vaccination rollout or earlier implementation of stricter NPIs (*e.g.*, expanding genomic testing to people entering from high-risk countries or elevating SD) resulted in less incidence, severe cases, and deaths. We are aware that the supply of vaccines is not enough globally, but fast administration of vaccines can block the occurrence of another wave. In other words, epidemic can be controllable and stable if the vaccination speed is faster.

There are several limitations of this research. First, the contact pattern in the transmission rate matrices already considers NPIs and might be not identical to the contact pattern before COVID-19, necessitating the normalization done on the matrices. For example, the transmission rate among those aged 0–17 might be underestimated because of restricted attendance in schools. Second, vaccine waning is not considered. However, booster shots are administered and vaccine hesitancy remains low in Korea, which mean that the effect of administered vaccines might be maintained [37]. Third, our age-age matrix focused on the Delta variant, and we were not able to examine transmission of other previous variants. The coverage of genomic surveillance among COVID-19 cases in Korea has steadily increased, and it covers about 30% of all confirmed cases. Therefore, the number of cases with genomic results before the occurrence of the Delta variant was small to be analyzed separately by variant types. Our results highlighted the transmission pattern of Delta, which is currently the dominant variant in most countries.

5. Conclusion

By developing transmission rate matrices based on MLE, this study showed the higher transmissibility of the Delta relative to the non-Delta variant among various age groups in Korea. The transmission rates were then used to quantify the effects of simultaneous NPIs and vaccination. The model simulation results emphasize the importance of concurrently applying interventions, such as SD, screening measures at the entry points, and vaccination. An epidemic wave can be avoided if a strict SD policy is not relaxed too early. Since the epidemic is still ongoing, transmission rate of the Delta variant of COVID-19 is high, and oral treatment is not yet widely available, we suggest that NPIs are still necessary to control the epidemic and reduce the number of severe cases in order to prevent overwhelming the healthcare system. Model simulations also showed that even with the same SD level, outcomes may change depending on vaccine administration and emergence of a highly transmissible variant. If vaccination is slow, then NPIs should be strictly implemented to lessen the medical and socio-economic burden of COVID-19 to the society.

Ethics approval

The study was conducted according to the guidelines of the Declaration of Helsinki, and approved by the Institutional Review Board of Konkuk University (7001355-202101-E-130)

Appendix A. Vaccine- and age-dependent parameter values

Table A.1 shows the effectiveness of one and two doses of ChAdOx1 and BNT162b2 to the non-Delta and Delta variants from [32]. These are the baseline values used to calculate the age-dependent e_i^{part} and e_i^{full} shown in Table A.2. The proportions of each age group administered with ChAdOx1 are also shown in Table A.2. The average interval between doses is set to 11 weeks for ChAdOx1 and 4 weeks for BNT162b2, according to KDCA policy [9]. We estimated the mean interval from first dose to immunity considering the vaccine effectiveness from first and second doses.

Let $\hat{e}_{c,1}$ and $\hat{e}_{c,2}$ ($\hat{e}_{b,1}$ and $\hat{e}_{b,2}$) be the vaccine effectiveness of ChAdOx1 (BNT162b2) from one and two doses, respectively. Then the expected proportion of vaccine effectiveness of first and second dose among effectively vaccinated hosts with ChAdOx1 (BNT162b2) are $\frac{\hat{e}_{c,1}}{\hat{e}_{c,1}+\hat{e}_{c,2}}$ and $\frac{\hat{e}_{c,2}}{\hat{e}_{c,1}+\hat{e}_{c,2}}$ ($\frac{\hat{e}_{b,1}}{\hat{e}_{b,1}+\hat{e}_{b,2}}$ and $\frac{\hat{e}_{b,2}}{\hat{e}_{b,1}+\hat{e}_{b,2}}$), respectively. Hence, if $\hat{P}_c$ is the proportion of hosts who were administered ChAdOx1 and assuming that the vaccinated hosts who did not have ChAdOx1 were given BNT162b2, the expected time to have immunity ($\hat{t}$) is given by

$$\hat{t} = \hat{P}_c\left(\frac{\hat{t}_{c,1}\hat{e}_{c,1}}{\hat{e}_{c,1}+\hat{e}_{c,2}} + \frac{\hat{t}_{c,2}\hat{e}_{c,2}}{\hat{e}_{c,1}+\hat{e}_{c,2}}\right) + (1-\hat{P}_c)\left(\frac{\hat{t}_{b,1}\hat{e}_{b,1}}{\hat{e}_{b,1}+\hat{e}_{b,2}} + \frac{\hat{t}_{b,2}\hat{e}_{b,2}}{\hat{e}_{b,1}+\hat{e}_{b,2}}\right),$$

where $\hat{t}_{\cdot,1}$ and $\hat{t}_{\cdot,2}$ indicate the time (in days) 2 weeks after first and second dose, respectively. Therefore, $\hat{t}_{c,1} = \hat{t}_{b,1} = 14$, $\hat{t}_{c,2} = 91$, and $\hat{t}_{b,2} = 42$ days. For example, value of $\hat{P}_c$ in age group 5 is 0.13. Considering vaccine effectiveness of ChAdOx1 and BNT162b2 for non-Delta are $\hat{e}_{c,1} = 0.487$, $\hat{e}_{c,2} = 0.745$, $\hat{e}_{b,1} = 0.475$, and $\hat{e}_{b,2} = 0.937$, $\hat{t}$ is estimated as 36.2184. Note that this value is slightly different from the value which was applied into model because we used the average value of $\hat{t}$ for non-Delta and Delta in each age group to get $1/\omega$.

Similarly, age-dependent vaccine effectiveness was calculated using the proportion of hosts who were administered with ChAdOx1 and BNT162b2. Assuming that everyone who is vaccinated will have a secondary dose,

Table A.1. Vaccine effectiveness of ChAdOx1 and BNT162b2 to the non-Delta and Delta variants depending on the number of doses [32].

	ChAdOx1		BNT162b2	
	First dose	Second dose	First dose	Second dose
Vaccine effectiveness to the non-Delta variant	0.487	0.745	0.475	0.937
Vaccine effectiveness to the Delta variant	0.300	0.670	0.356	0.880

Table A.2. Proportion of age group i administered with ChAdOx1 from data [5] and the calculated age-dependent vaccine effectiveness to the Delta and non-Delta variants, and average duration to develop full immunity.

Description	Age group							
	1	2	3	4	5	6	7	8
Proportion of age group i administered with ChAdOx1	0.00	0.03	0.15	0.21	0.13	0.93	0.55	0.11
e_i^{part}	0.94	0.93	0.91	0.9	0.91	0.76	0.83	0.92
e_i^{full}	0.88	0.87	0.85	0.84	0.85	0.69	0.76	0.86
$1/\omega_i$ (days)	33.26	34.18	37.85	39.69	37.24	61.73	50.10	36.63

the vaccine effectiveness is obtained as follows,

$$e_i = \hat{P}_c \hat{e}_{c,2} + (1 - \hat{P}_c)\hat{e}_{b,2}.$$

Appendix B. Calculation of the basic reproductive number

The basic reproductive number, denoted by $\mathcal{R}_0$, is the number of secondary cases produced in a completely susceptible population by an initial infectious individual over the course of its infectious period. In this research, we used the next generation method [41] to calculate the basic reproductive number with the transmission rate matrix. Note that the vaccine terms, variant-related model variables, and NPIs-reduction factor are ignored. The system variables and its derivatives are expressed as vector form as follows;

$$\begin{aligned} \mathbf{S} &= (S_1, \ldots, S_8)^t, \quad & \mathbf{S}' &= \frac{\mathrm{d}\mathbf{S}}{\mathrm{d}t}, \\ \mathbf{E} &= (E_1, \ldots, E_8)^t, \quad & \mathbf{E}' &= \frac{\mathrm{d}\mathbf{E}}{\mathrm{d}t}, \\ \mathbf{I} &= (I_1, \ldots, I_8)^t, \quad & \mathbf{I}' &= \frac{\mathrm{d}\mathbf{I}}{\mathrm{d}t}. \end{aligned}$$

Considering the disease-free equilibrium,

$$\begin{aligned} \mathbf{S^0} &= (N_1, \ldots, N_8)^t, \\ \mathbf{E^0} &= (0, \ldots, 0)^t, \\ \mathbf{I^0} &= (0, \ldots, 0)^t, \end{aligned}$$

where N_i indicate the original population size of age group i. Linearizing the system at the disease free equilibrium state can be described with a vector derivative form in matrix as follows;

$$M = \begin{bmatrix} \frac{\partial \mathbf{E}'}{\partial \mathbf{E}} & \frac{\partial \mathbf{E}'}{\partial \mathbf{I}} \\ \frac{\partial \mathbf{I}'}{\partial \mathbf{E}} & \frac{\partial \mathbf{I}'}{\partial \mathbf{I}} \end{bmatrix},$$

and $(\mathbf{S}, \mathbf{E}, \mathbf{I}) = (\mathbf{S^0}, \mathbf{E^0}, \mathbf{I^0})$. Matrix M is divided into two matrices F and V, *i.e.*, $M = F - V$, where F refers to the rate of appearance of new infections in the compartments and V refers to the rate of transfer of individuals. Multiplication of F and V^{-1}, FV^{-1}, is as follows,

$$FV^{-1} = \begin{bmatrix} T_1 & T_2 \\ T_3 & T_4 \end{bmatrix},$$

where each of the blocks T_1, T_2, T_3 and T_4 are 8-by-8 matrices. The matrices T_3 and T_4 are zero matrices, while T_1 and T_2 indicate the ratio between the inflow and outflow of exposed groups, which is the next generation matrix G, $G = T_1 = T_2$, then

$$G[i, j] = \frac{\beta_{ij}}{\alpha} \frac{N_i}{\sum_k N_k}.$$

The matrix FV^{-1} has (i, j) entry which is the expected number of secondary infections in i by infector j. Thus, the basic reproductive number ($\mathcal{R}_0$) is the spectral radius of FV^{-1}, written as

$$\mathcal{R}_0 = \rho\big(FV^{-1}\big).$$

Acknowledgements. This paper is supported by the Korea National Research Foundation (NRF) grant funded by the Korean government (MEST) (NRF-2021M3E5E308120711). This paper is also supported by the Korea National Research Foundation (NRF) grant funded by the Korean government (MEST) (NRF-2021R1A2C100448711).

References

[1] Centers for Disease Control and Prevention, National Center for Immunization and Respiratory Diseases (NCIRD), Division of Viral Diseases, U.S. Science Brief: COVID-19 Vaccines and Vaccination, https://www.cdc.gov/coronavirus/2019-ncov/science/science-briefs/fully-vaccinated-people.html, accessed: October 6, 2021.

[2] COVID-19 Vaccination status, https://ncv.kdca.go.kr/eng/, accessed: April 13, 2022.

[3] Korea Disease Control and Prevention Agency, Anounce about the adjustement of social distancing, http://ncov.mohw.go.kr/infoBoardView.do?brdId=3&brdGubun=32&dataGubun=&ncvContSeq=6009&contSeq=6009&board_id=&gubun=, accessed: October 14, 2021.

[4] Korea Disease Control and Prevention Agency; Korean situation report of COVID-19; 2021 October 27, http://ncov.mohw.go.kr/tcmBoardView.do?brdId=3&brdGubun=31&dataGubun=&ncvContSeq=6043&contSeq=6043&board_id=312&gubun=ALL, accessed: October 27, 2021.

[5] Korea Disease Control and Prevention Agency; Korean situation report of COVID-19; 2021 October 8, http://ncov.mohw.go.kr/tcmBoardView.do?brdId=3&brdGubun=31&dataGubun=&ncvContSeq=5989&contSeq=5989&board_id=312&gubun=ALL, accessed: October 14, 2021.

[6] Korea Disease Control and Prevention Agency; Proportions of variants among sampled genome sequencing in Korea, https://kdca.go.kr/contents.es?mid=a20107040000, accessed: October 27, 2021.

[7] Korea Disease Control and Prevention Agency, PUBLIC HEALTH WEEKLY REPORT, PHWR (Vol.14, No.17, 2021), https://www.kdca.go.kr/board/board.es?mid=a30501000000&bid=0031&list_no=713112&act=view, accessed: October 21, 2021.

[8] Korea Disease Control and Prevention Agency, PUBLIC HEALTH WEEKLY REPORT, PHWR (Vol.14, No.37, 2021), https://www.kdca.go.kr/board/board.es?mid=a30501000000&bid=0031&list_no=716914&act=view#, accessed: October 21, 2021.

[9] Korea Disease Control and Prevention Agency, Questions and answers about COVID-19 vaccines, criteria for the implementation of COVID-19 vaccination, https://ncv.kdca.go.kr/menu.es?mid=a12207000000, accessed: October 14, 2021.

[10] Korea Disease Control and Prevention Agency; Who will have vaccine first?, https://ncv.kdca.go.kr/menu.es?mid=a10117010000, accessed: October 14, 2021.

[11] Ministry of Education, Announce about school operation plan after Chuseok holiday, https://www.korea.kr/news/policyNewsView.do?newsId=148878606, accessed: October 14, 2021.

[12] Ministry of Health and Welfare, Republic of Korea. Coronavirus disease 2019 (COVID-19), http://ncov.mohw.go.kr/en/, accessed: October 6, 2021.

[13] National Institute for Mathematical Sciences, COVID-19 forecasts using mathematical modeling, https://www.nims.re.kr/research/post/covid19_2/34405, accessed: October 14, 2021.

[14] The Ministry of Health and Welfare, Plan of the step-by-step recovery from COVID-19, http://www.mohw.go.kr/react/al/sal0301vw.jsp?PAR_MENU_ID=04&MENU_ID=0403&page=1&CONT_SEQ=368237, accessed: October 14, 2021.

[15] WHO Situation Reports, https://www.who.int/publications/m/item/weekly-epidemiological-update-on-covid-19—5-october-2021, accessed: October 6, 2021.

[16] YTN science, Delta variant takes 96.7% among variants and number of cases for a week was 2555, 7467 in total, https://science.ytn.co.kr/program/program_view.php?s_mcd=0082&key=202108101604183996&page=2, accessed: October 14, 2021.

[17] J.P. Arcede, R.L. Caga-Anan, C.Q. Mentuda and Y. Mammeri, Accounting for symptomatic and asymptomatic in a SEIR-type model of COVID-19. *Math. Modell. Nat. Phenom.* **15** (2020) 34.

[18] E. Augeraud-Véron, Lifting the COVID-19 lockdown: different scenarios for France. *Math. Modell. Nat. Phenom.* **15** (2020) 40.

[19] L. Bian, Q. Gao, F. Gao, Q. Wang, Q. He, X. Wu, Q. Mao, M. Xu and Z. Liang, Impact of the Delta variant on vaccine efficacy and response strategies. *Exp. Rev. Vacc.* **0** (2021) 1–9.

[20] G. Bianchin, E. Dall'Anese, J.I. Poveda, D. Jacobson, E.J. Carlton and A.G. Buchwald, Novel use of online optimization in a mathematical model of COVID-19 to guide the relaxation of pandemic mitigation measures. *Sci. Rep.* **12** (2022) 1–14.

[21] M.A. Billah, M.M. Miah and M.N. Khan, Reproductive number of coronavirus: a systematic review and meta-analysis based on global level evidence. *PloS One* **15** (2020) e0242128.

[22] F. Campbell, B. Archer, H. Laurenson-Schafer, Y. Jinnai, F. Konings, N. Batra, B. Pavlin, K. Vandemaele, M.D. Van Kerkhove, T. Jombart *et al.*, Increased transmissibility and global spread of SARS-CoV-2 variants of concern as at June 2021. *Eurosurveillance* **26** (2021) 2100509.

[23] G. Chowell, Fitting dynamic models to epidemic outbreaks with quantified uncertainty: a primer for parameter uncertainty, identifiability, and forecasts. *Infect. Disease Model.* **2** (2017) 379–398.

[24] K. Dougherty, M. Mannell, O. Naqvi, D. Matson and J. Stone, SARS-CoV-2 B. 1.617. 2 (Delta) variant COVID-19 outbreak associated with a gymnastics facility—Oklahoma, April–May 2021. *Morb. Mort. Weekly Rep.* **70** (2021) 1004.

[25] J. Jang, M.-J. Hwang, S.Y. Park, S.-S. Kim, J. Park, H. Yeom, S.B. Park and K. Donghyoks, Trends in COVID-19 cases among children and adolescents aged 0-18 years in the Republic of Korea. *Korea Dis. Control Prev. Agency: Weekly Health Dis.* **14** (2021).

[26] M.J. Keeling, E.M. Hill, E.E. Gorsich, B. Penman, G. Guyver-Fletcher, A. Holmes, T. Leng, H. McKimm, M. Tamborrino, L. Dyson *et al.*, Predictions of COVID-19 dynamics in the UK: Short-term forecasting and analysis of potential exit strategies. *PLoS Comput. Biol.* **17** (2021) e1008619.
[27] M. Ki *et al.*, Epidemiologic characteristics of early cases with 2019 novel coronavirus (2019-nCoV) disease in Korea. *Epidemiol. Health* **42** (2020).
[28] Y. Ko, J. Lee, Y. Kim, D. Kwon and E. Jung, COVID-19 vaccine priority strategy using a heterogenous transmission model based on maximum likelihood estimation in the Republic of Korea. *Int. J. Environ. Res. Public Health* **18** (2021) 6469.
[29] Y. Ko, J. Lee, Y. Kim, D. Kwon and E. Jung, COVID-19 vaccine priority strategy using a heterogenous transmission model based on maximum likelihood estimation in the Republic of Korea. *Int. J. Environ. Res. Public Health* **18** (2021) 10.3390/ijerph18126469.
[30] Y. Ko, J. Lee, Y. Seo and E. Jung, Risk of COVID-19 transmission in heterogeneous age groups and effective vaccination strategy in Korea: a mathematical modeling study. *EpiH* (2021).
[31] Y.-H. Lee, C.M. Hong, D.H. Kim, T.H. Lee and J. Lee, Clinical course of asymptomatic and mildly symptomatic patients with coronavirus disease admitted to community treatment centers, South Korea. *Emerg. Infect. Dis.* **26** (2020) 2346.
[32] J. Lopez Bernal, N. Andrews, C. Gower, E. Gallagher, R. Simmons, S. Thelwall, J. Stowe, E. Tessier, N. Groves, G. Dabrera *et al.*, Effectiveness of Covid-19 vaccines against the B. 1.617. 2 (Delta) variant. *N. Engl. J. Med.* (2021) 585–594.
[33] E. Mahase, Delta variant: What is happening with transmission, hospital admissions, and restrictions? (2021).
[34] S. Marino, I.B. Hogue, C.J. Ray and D.E. Kirschner, A methodology for performing global uncertainty and sensitivity analysis in systems biology. *J. Theor. Biol.* **254** (2008) 178–196.
[35] A. Moussaoui and P. Auger, Prediction of confinement effects on the number of Covid-19 outbreak in Algeria. *Math. Model. Nat. Phenom.* **15** (2020) 37.
[36] H. Nishiura and G. Chowell, The Effective Reproduction Number as a Prelude to Statistical Estimation of Time-Dependent Epidemic Trends, 103–121, Springer Netherlands, Dordrecht (2009).
[37] H.K. Park, J.H. Ham, D.H. Jang, J.Y. Lee and W.M. Jang, Political ideologies, government trust, and COVID-19 VACCINE HESITANCY in South Korea: a cross-sectional survey. *Int. J. Environ. Res. Public Health* **18** (2021) 10655.
[38] T.A. Perkins and G. España, Optimal control of the COVID-19 pandemic with non-pharmaceutical interventions. *Bull. Math. Biol.* **82** (2020) 1–24.
[39] G. Rainisch, E.A. Undurraga and G. Chowell, A dynamic modeling tool for estimating healthcare demand from the COVID19 epidemic and evaluating population-wide interventions. *Int. J. Infectious Dis.* **96** (2020) 376–383.
[40] R. Rowthorn and J. Maciejowski, A cost–benefit analysis of the COVID-19 disease. *Oxford Rev. Econ. Policy* **36** (2020) S38–S55.
[41] P. Van den Driessche and J. Watmough, Reproduction numbers and sub-threshold endemic equilibria for compartmental models of disease transmission. *Math. Biosci.* **180** (2002) 29–48.
[42] Y. Wang, R. Chen, F. Hu, Y. Lan, Z. Yang, C. Zhan, J. Shi, X. Deng, M. Jiang, S. Zhong *et al.*, Transmission, viral kinetics and clinical characteristics of the emergent SARS-CoV-2 Delta VOC in Guangzhou, China. *EClinicalMedicine* **40** (2021) 101129.
[43] WHO *et al.*, Transmission of SARS-CoV-2: implications for infection prevention precautions: scientific brief, 09 July 2020. Tech. rep., World Health Organization (2020).
[44] J. Yang, G. Wang, S. Zhang, F. Xu and X. Li, Analysis of the age-structured epidemiological characteristics of SARS-COV-2 transmission in mainland China: an aggregated approach. *Math. Modell. Nat. Phenom.* **15** (2020) 39.
[45] K. Youngwha, K. Yuyeon, H. Yum, J. Jang, I. Hwang, G. Park, Y. Park, S. Lee and D. Kwon, Annual COVID-19 occurrence report. *Korea Disease Control and Prevention Agency: Weekly health and diseases* **14** (2021).